THE AUTHOR

John K. Gillham received his Bachelor of Arts in Natural Sciences from Cambridge University in 1953 and the Ph.D. in Chemistry from McGill University in 1959. He spent six years at the Stamford Research Laboratories of the American Cyanamid Company working on new polymers. A year's leave spent in the Department of Chemical Engineering at Princeton University was followed by his joining that department where he is an associate professor. His teaching and research responsibilities are in the field of polymeric materials. He is involved in the commercialization of his TBA technique and in consulting with the Polymer Industry.

Development of the TBA technique has not been without the raised eyebrows of colleagues; appellations have included, "Wet Sock Technique" and, more politely, "Chemistry on a String." The synthetic polymer chemist has been interested in his molecules as molecules, whereas the polymer physicist is content to spend his life with polystyrene. John Gillham covers the territory in between.

Dynamic Meniscus Profiles in Free Coating III Predictions Based on Two-Dimensional Flow Fields

CHIE Y. LEE
and
JOHN A. TALLMADGE

Department of Chemical Engineering
Drexel University
Philadelphia, Pennsylvania, 19104

One challenging problem in liquid-gas, interfacial phenomena is the prediction of the size and location of a flowing meniscus because it involves surfaces which are highly curved. The paper presents one aspect of this problem. A numerical method is presented for predicting the dynamic meniscus profiles—specifically those distorted considerably by flow. The geometry considered to provide these free (liquid-gas) surfaces is coating of a moving sheet by upward withdrawal from a finite bath. The predicted profiles agree with data taken with a glycerine-water solution and with viscous oils.

The method predicts the three parameters (coating thickness and two others) which are the minimum number of parameters necessary to describe the dynamic-meniscus profiles for this geometry. The numerical method is iterative, it simultaneously predicts the flow field in the bath, and it is based on the two-dimensional Navier-Stokes equations and appropriate boundary conditions. The interfacial boundary condition used for iteration is the normal stress condition which is composed of pressure, surface tension, and viscous terms.

SCOPE

This paper is concerned with the simultaneous prediction of dynamic meniscus profiles and flow fields in free coating of sheets by withdrawal from finite baths. The free coating geometry has been used commercially for photographic emulsions, galvanized steel, drawn glass plates, electroplating rinses, and other applications and is often followed by a film reduction device. In these and other coating geometries, there is a need for minimizing coating nonuniformities. The study of dynamic meniscus profiles and their flow fields is considered relevant to understanding the nature of flow instabilities, which in turn are believed to give rise to film nonuniformities.

The first objective of this paper is to present a numerical technique, based on two-dimensional flow, for predicting the dynamic meniscus profiles in terms of three parameters, the film coating thickness and the size and shape of the meniscus. The technique simultaneously predicts the flow fields and involves a search for minimum error in terms of two parameters which are related to shape and coating thickness. The error is calculated using a pressure error integral over the meniscus, which is based on the normal stress boundary condition along the meniscus interface. The major subroutine is a stream function-vorticity iteration for each assumed profile.

Most previous theoretical work in free coating has concentrated on the prediction of one dependent variable, coating thickness, as a function of one independent variable, the capillary number. The method described in this paper describes the prediction of three dependent parameters as a function of four independent parameters; the latter are Reynolds number Re, capillary number Ca, bath depth, and bath width.

The second objective of this paper is to compare the predicted results with experimental profiles, using data obtained from photographs of coating on a continuous belt device.

Correspondence concerning this paper should be addressed to J. A. Tallmadge. C. Y. Lee is with DeLaval Corporation, Pleasant Valley, New York.

CONCLUSIONS AND SIGNIFICANCE

Predicted profiles were found to agree with profile data within experimental error at capillary above one. Results of the numerical method compared favorably with profile data for a glycerine-water solution with a viscosity of 0.86 N-s/m^2 taken at a speed of 143 mm/s in a bath having depth and width of 40 × 65 mm. For these conditions, Ca was 2.1 and Re was 0.7. Numerical results also compared favorably with runs with two viscous oils at coating speeds ranging from 75 to 680 mm/s; for these conditions Ca ranged from 3 to 24 and Re from 0.2 to 13. The method is currently useful for all Re up to 13 or higher and for Ca above one. Extension to lower Ca may be possible.

The method predicts how the size of dynamic menisci increases at larger coating speeds and viscosities, decreases with small bath depths, and changes with other fluid properties. Also predicted are the relative sizes of the normal forces which occur along the curved surface; these forces include those of pressure, surface tension, and viscous. It is believed that the numerical technique can be applied to other geometries for cases where the functional form of the meniscus profiles is understood.

The problem of nonuniform liquid films arises in many applications, including bead and slide coating, transfer-roll coating, and free coating. The nonuniformities are due in part to flow instabilities and may include the shedding of vortices from menisci. These nonuniformities may appear as film waves (Tallmadge and Soroka, 1969), bath waves (Gutfinger, 1964), or cross-streaks and ridge lines (Tuntiblarphol, 1970). Some of these phenomena have not been described by predictions, partly because most existing entrainment theories are based on pseudo one-dimensional models (Groenveld, 1970; Landau and Levich, 1942). It is felt, therefore, that two-dimensional flow descriptions would be helpful to understand these phenomena.

In many coating applications, a dynamic meniscus is present which may influence film uniformity. For these and other reasons, the authors are interested in describing the curved surfaces and capillary forces present in flowing menisci. In particular, the authors are interested in predicting the flow fields near menisci and in predicting the profiles of curved, interfacial boundaries which arise in meniscus flow.

DESCRIPTION OF THE WITHDRAWAL COATING PROBLEM

The geometry of interest for this paper is the free coating of a flat sheet from a finite bath, as shown in Figure 1. This geometry was chosen because of prior work on it by the authors. When a continuous flat plate of a given width is withdrawn vertically and continuously at a constant velocity u_w from a finite liquid bath having a depth d and a width w, a film of the liquid will adhere to the plate. As shown in Figure 1, the meniscus thickness h of the adhering film will decrease from that at the bath liquid level to a constant thickness h_0. At a position near the moving sheet, the stream lines are nearly parallel to the sheet and the flow is upward because of the pumping action of the solid surface. This process is called *free coating by withdrawal.*

Because a portion of liquid usually flows back down to the liquid bath, there is an upper stagnation point B, at which the reverse flow occurs. A second (lower) stagnation point occurs at some point C. On the upper meniscus surface AB the liquid flow is upward and on the lower meniscus surface BC the liquid flow is downward. In this paper, the fluid is incompressible and the flow is Newtonian, laminar, stable; the solid support is completely wet by the fluid; and gravity is the only body force.

The case considered here is steady flow, where the amount of liquid added to the right corner of bath is equal to that withdrawn by coating. This feed flow maintains the liquid level constant. Since flow is downward near the liquid inlet, an eddy is created in the lower right corner of the bath and a vortex is usually created in the bath below BC.

The characteristic length is given by $h_c \equiv (\mu u_w/\rho g)^{1/2}$. In nondimensional terms, the coating speed, inertial force, bath depth, and bath width are given respectively by the capillary number $Ca \equiv u_w(\mu/\sigma)$, the Reynolds number $Re \equiv u_w(\rho h_c/\mu)$, depth $(D = d/h_c)$, and width $(W = w/h_c)$. Some of the dependent variables are meniscus profiles $h(x)$ and flow field $u(x, y)$ and $v(x, y)$. One important part of the profile is the coating thickness h_0, which occurs in the constant thickness region. The nondimensional coating thickness is T_0, which is nearly constant at 0.6 to 0.8 for most of the conditions considered herein. The coating thickness has been described theoretically as a function of capillary number by several authors, including Landau and Levich (1942) and Groenveld (1970).

MENISCUS PROFILES (LITERATURE)

Based on data, there is some understanding of the form of the $h(x)$ profiles and the dependence of the profiles on coating parameters. For example, complete profiles for dynamic menisci of the type shown in Figure 2a have been measured. These profiles have been linearized using

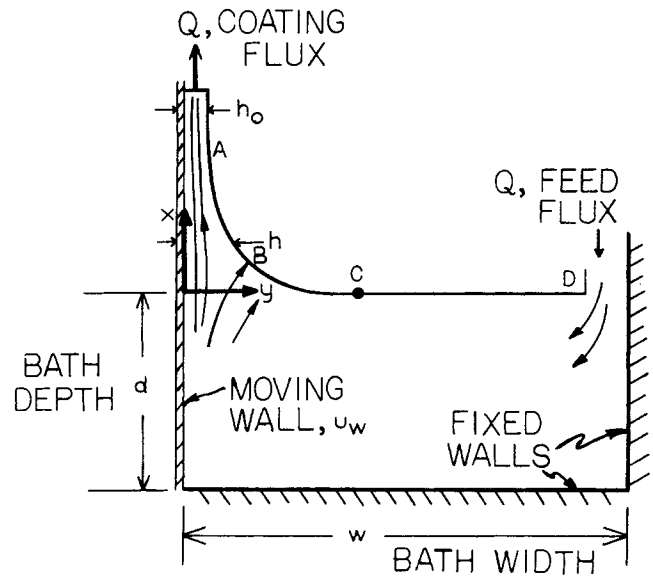

Fig. 1. A sketch of the free coating withdrawal process.

semilog plots, as shown in Figures 2b and 2c. Figure 2b shows the plot of log $(h - h_0)$ and Figure 2c shows the profile in the nondimensional terms of meniscus thickness $L \equiv h/h_0$ and meniscus height $\lambda \equiv x/h_0$. Data for meniscus profiles in nondimensional form have been described analytically (Lee and Tallmadge, 1972b, 1973a) by the following expression:

$$L \equiv (h/h_0) = 1 + B \exp[-x/Mh_0] \qquad (1)$$

or

$$\lambda = (M \ln B) - M \ln (L - 1) \qquad (1A)$$

For each profile, there are three parameters: T_0 (the coating thickness), M (the slope in Figure 2c), and B. Here M is associated with the shape of the meniscus and B is associated with the horizontal intercept (Figure 2c) and thus the size of the meniscus. The M and B parameters used here are those obtained from the thick region of the menisci, which were called M_2 and B_2 by Lee and Tallmadge (1973a).

Tabular values of experimental meniscus profiles, in terms of the three profile parameters, have been given for one viscous oil at several coating speeds and bath depths (Lee and Tallmadge, 1973a). The work on complete profiles was stimulated by earlier work by Groenveld and Van Dortmund (1970) on the upper portion of the film, shown as AB in Figure 1, where the film is thin and has small curvatures.

A theoretical prediction of meniscus profiles has recently been developed, based on models of pseudo one-dimensional flow in the meniscus (Lee et al., 1972; Lee, 1974). The results of these one-dimensional models agree closely with the data in terms of functional form [Equation (1)] and agree approximately in terms of the slope (M). However, both one-dimensional models underestimate the magnitude or size of dynamic menisci by a considerable amount; that is, the value of intercept B is underestimated considerably. This limitation on the one-dimensional results confirms that a two-dimensional flow approach is desirable. Such a two-dimensional study offers the potential of improved prediction of the meniscus profiles (specifically size) and a more reliable description of the flow problem.

One of the one-dimensional flow models for predicting profiles utilized the flow form of the normal stress boundary condition (Batchelor, 1967), which is

$$p_G - p_L = \sigma c + 2\mu \left[\frac{\partial u_s}{\partial s} \right]_n \qquad (2)$$

For small viscosity and surface velocities, Equation (2) reduces to the well-known Laplace equation of capillary statics, which was used for the other model:

$$p_G - p_L = \sigma c = \sigma \frac{d^2h/dx^2}{[1 + (dh/dx)^2]^{1/2}} \qquad (2A)$$

DISCUSSION OF APPROACH FOR TWO-DIMENSIONAL FLOW

There are several forces involved in the free coating process, namely viscous, gravitational, inertial, and pressure (or surface tension). The principal difficulty encountered in the analysis here is the problem of predicting a highly-curved profile of a (free) surface of unknown location simultaneously with the flow field (Soroka, 1969). The generation of a numerical solution for one specific set of flow conditions is difficult since the position of the interfacial (free) boundary is not known.

Existing analytical and numerical methods were surveyed, but all have some difficulty when applied to the geometry given in Figure 1. For example, the particle-and-cell method (Hirt, 1970; Churchill and Wellington, 1972) is limited to small curvatures and requires long times for computation of steady state. Another method uses a protean coordinate transformation (Duda and Vrentas, 1967), but it can not be applied to the vortex flow shown in Figure 1 because of double valued functions.

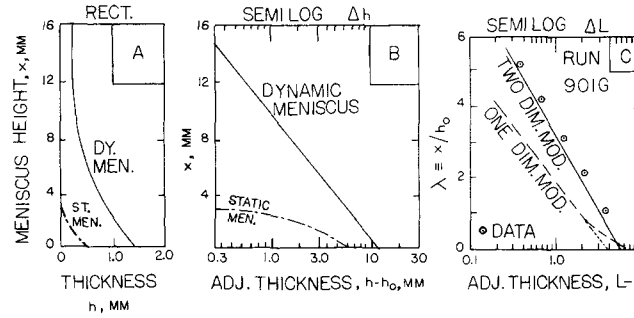

Fig. 2. Meniscus profiles in free coating: (Part A—A rectangular plot), (Part B—A dimensional semilog plot), (Part C—Comparison with glycerine data run 901G).

To overcome the free surface difficulty, the following strategy was developed and used by the authors: (Lee and Tallmadge, 1973b)

(Part 1) Using an assumed position of the free surface $h(x)$, the equations of motion expressed in terms of the vorticity and stream function were solved numerically by modifying standard methods. (Lee and Talmadge, 1972a)

(Part 2) Using the normal stress boundary condition as a criterion to be satisfied all along the free surface, an error integral was defined and evaluated numerically from the assumed profile of Part 1.

(Part 3) Using the error integral, the assumed profile was improved and optimized by iteration to the desired precision.

The third part requires iteration of an unknown profile $h(x)$. In numerical form, this profile can be represented, in general, by a number of discrete points in a tabular array (Soroka, 1969). Because of the large curvatures present, a large number of points would be needed to yield precise values of the higher derivatives present in $(p_G - p_L)$ and dp/dx. To overcome the problem of iterating a large number of points for an unknown profile function, the authors also used two additional strategies:

(Part 4) An analytical form was selected to express the complete profile with a small number of parameters.

(Part 5) As a first test of the method, the minimum number of parameters necessary was selected. The minimum number is three, one for coating thickness and two for a linear representation of the profile region. The meniscus expression given by Equation (1) was selected because it is the approximation which is most accurate in size h for the entire profile. Thus the three nondimensional parameters to be optimized are thickness T_0, slope M, and intercept B. The quantity B is only approximate for the point at liquid bath level.

In summary, this approach separates the analysis into two iterations given by Parts 1 and 3. First, the flow field is determined for a given surface (that is, for given M, B, T_0) and second, the profile parameters are optimized using part 1 as a numerical subroutine. The technique is essentially a double or nested iteration.

These five strategies were developed in a complex, simultaneous process. In this process, several results were obtained which are important in themselves. Such results include those for profile data (Lee and Tallmadge, 1972b, 1973a), one-dimensional models (Lee et al., 1972; Lee, 1973) and vortexing (Lee and Tallmadge, 1972a). The authors wish to emphasize that these results were also preliminary to, and an important part of, development of the method described above in this paper.

FLOW FIELD FOR A GIVEN PROFILE (PART 1)

The prediction of stream lines, vorticity, and stagnation points in free coating for a given profile has been published previously, along with confirming data (Lee and Tallmadge, 1972a). See the Appendix. Thus Part 1 is available elsewhere. One of the equations of constraint used earlier was the "given" profile, indicated by Equation (3)

$$h = h(x) \text{ given} \tag{3}$$

In this paper, constraint Equation (3) will be replaced by a normal-stress equation as noted below.

CRITERION FOR IMPROVING THE ASSUMED MENISCUS PROFILE (PART 2)

In place of the assumed profile [Equation (3)], a two-dimensional flow prediction will be presented in this section which uses the normal stress condition of Equation (2) as a boundary condition. In order to predict the meniscus profile, the flow field will be determined simultaneously. The normal stress boundary condition for a liquid-gas free surface, given by Equation (2), was placed in nondimensional form by multiplying by $h_c/(\mu u_w)$ to obtain

$$\frac{h_c \Delta p}{\mu u_w} \equiv \Delta P = \frac{C}{Ca} + \frac{2\partial U_s}{\partial S} \tag{4}$$

The pressure profile $\Delta_B(x)$ which results from an assumed profile is, in general, different from the precise desired profile ΔP for any set of conditions. The former was determined by evaluating the curvature term analytically and the flow term numerically in finite difference form using ΔU_s and ΔS and combining to obtain $\Delta_B(x)$ as follows:

$$\Delta_B(X) = \frac{C}{Ca} + \frac{2\partial U_s}{\partial S} \tag{5}$$

Another estimate of the pressure profile $\Delta_F(x)$ was obtained by evaluating $\partial P/\partial X$ and $\partial P/\partial Y$ at the interface (based on the flow field values of stream function and vorticity) and using the finite difference form of the following equation:

$$\Delta_F(X) = \int \frac{\partial P}{\partial Y} dY + \int \frac{\partial P}{\partial X} dX \tag{6}$$

The difference between the two estimates of the pressure profiles at the interface is the pressure error profile $E(X)$ given by

$$E(X) = \Delta_F(X) - \Delta_B(X) \tag{7}$$

The pressure error integral R was defined as the integral of the absolute value of E or

$$R \equiv \int_{X_1}^{X_2} |E(X)| dx \tag{8}$$

Here the X_1 integration limit was taken at the constant thickness region ($L = 1$) and X_2 was taken at the bath surface ($L = 1 + B$). Numerically, the error was calculated by difference on each node point along the free surface, using the vertical X direction and a constant distance ΔX.

The minimum value of the error integral was used as the criterion for iteration in this work. Other types of criterion were considered, including integration of E over dy or ds, but no appreciable differences were found. The dx variable was selected because it is more convenient with the numerical scheme used.

As an example for these functions, consider the conditions of glycerine run 901G (Lee and Tallmadge, 1972a) for which the independent parameters were thickness $h_c = 3.16$ mm, $Ca = 2.1$, $Re = 0.66$, $D = 12.7$, and $W = 20.6$. For an assumed profile ($T_0 = 0.68$, $M = 1.85$, and $B = 5.7$), the resultant profiles for Δ_F, Δ_B, and E are shown in Figure 3—as parts A, B, and C, respectively. The abscissa is the nondimensional thickness L, which has a maximum value equal to $(B + 1)$.

Figures 3a and 3b show that, for the run studied, the functions Δ_F and Δ_B are similar in size and shape. Figure 3b shows that the viscous term is larger at a Ca of 2.1 (and a Re of 0.66) than the curvature term for most of the interface. The error function of Figure 3c is typical of those calculated in this work where errors were rather small.

SEARCH FOR THE PROFILE (PART 3)

The problem of predicting the meniscus profile along with the flow field is now a problem of predicting the three parameters (M, B, T_0) which result in a minimum error integral for a given set of four conditions, that is, for given Ca, Re, bath depth, and bath width. Using exploratory calculations with assumed profiles in the Ca range of 10^{-1} to 10^{+1} and the Re range of 10^{-2} to 10^{+1}, it was found that the error integral is most sensitive to changes in thickness T_0 and slope M, but is relatively insensitive to changes in intercept B. Considerable interaction between thickness and slope was noted. Based on the preliminary tests, the following iteration technique to minimize the residual error was developed and used to predict values of M, B, and T_0.

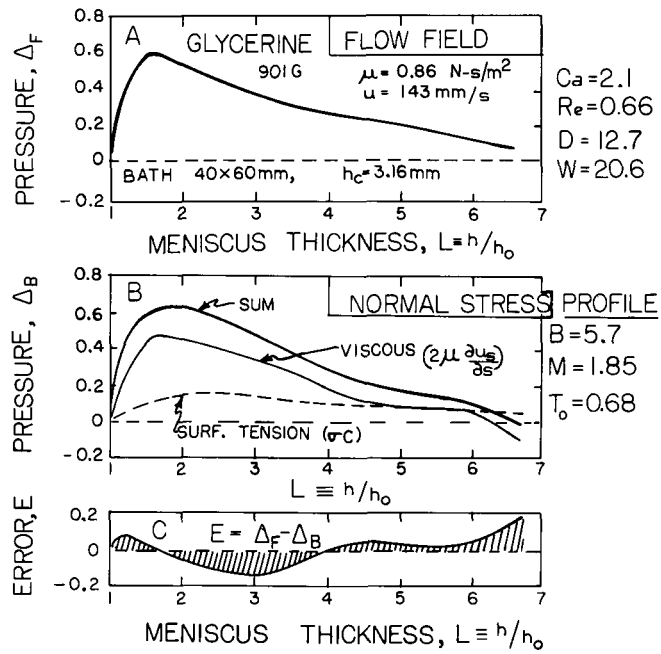

Fig. 3. Calculated pressure profiles and the error profile: (For condition of glycerine run 901G), (For Ca of 2.1, Re of 0.66, D of 12.7), (At B of 5.7, M of 1.85, T_0 of 0.68).

1. Assume a T_0, M, and B for a given condition.
2. Obtain the numerical solution for stream and vorticity functions as described previously.
3. Calculate the vortex center location H_v in terms of horizontal distance Y between the center of the vortex cell and the moving sheet.
4. Adjust the intercept B by taking B as equal to H_v.
5. Calculate the pressure error integral, as noted above.
6. Adjust the slope M and thickness T_0, based on the error integral.
7. Repeat all the calculations from Step 2 on until the error integral is a minimum within the desired precision in M and T_0.

The intercept B was taken as equal to the vortex center H_v because calculated B values appeared to occur at locations which were nearly identical to the center of the vortex cell and because B was found to be nearly constant for a wide range of M and T_0 values.

The step four strategy developed for the intercept B simplified a three-parameter search for slope and thickness (M and T_0). Because of this, the step four method for the intercept B led to a considerable reduction in computation time and simplified convergence. Although the procedure has not been justified rigorously, it does have some physical explanation. For example, as implied in Figure 1, the flow on the left of vortex center is upward and the flow on the right of the vortex center is downward. Thus, in one sense, the size of the meniscus near the liquid level of the bath, as given by intercept B, corresponds to the location of vortex center.

For an example of the two parameter search, consider glycerine run 901G, for which bath size and other run conditions (h_c, Ca, and Re) are given in the preceding section. For these conditions, the method described here predicted that intercept $B = 5.7$ (for a wide range of conditions), slope $M = 1.85$ within 3%, and thickness $T_0 = 0.68$ within 6%. Thus the numerical method of this work predicts that Equation (1) has the following parameters for run 901G:

$$L \equiv (h/h_0) = 1 + 5.7 \exp(x/1.85\, h_0) \qquad (9)$$

here

$$h_0 \equiv T_0 h_c = 0.68\, h_c \qquad (9A)$$

Because the functional dependence of the error integral on M and T_0 is of interest for future workers, an example is shown in Table 1 for the conditions of glycerine run 901G. Table 1 shows that the R function has a valley running at a large angle to both the T_0 and M axes so that an angular ridge line was present. Much larger values of the error were obtained at larger and smaller values of slopes and thicknesses. Table 1 shows a coarse grid using a 10% increment in M and, because R is more sensitive to T_0, a 5% increment in T_0. Halving the grid size to obtain a fine grid results in values of R shown in Table 2.

In this work, the increments were stopped as shown in Table 2 so that T_0 and M were predicted within about 3% and 6%, respectively, which is less than the uncertainty in the experimental error. Table 2 shows the evidence for the predicted values of M and T_0, which are given in Equations (9) and (9a) above.

For run 901G, the two-parameter search was done manually. With other runs, it was found that a good set of modified values were obtained quickly, without a lot of iteration steps, by adjusting the slope M using the pressure error on the upper, or small L, portion of the meniscus (increase the slope if the error is positive) and adjusting the thickness T_0 using the pressure error on the bottom portion of the meniscus (increase the thickness if the error is positive). Recommendations for initial estimates to use for B, M, and T_0 have been developed by Lee (1974) as functions of one or more of the four independent parameters (Ca, Re, D, and W).

Table 1. Coarse Grid Values of the Pressure Error Integral, R. Influence of Slope and Thickness on the Pressure Error[a,c]

Parameters				
Slope (M):	1.62	1.76	1.92[b]	2.13
Thickness (T_0)		Values of error integrals, $R \times 100$		
0.602	16.0	—	—	—
0.633	12.3	12.6	—	—
0.665	13.0	8.0	9.9	23.0
0.697[b]	—	10.8	7.5[b]	13.0
0.729	—	—	14.6	16.5
0.760	—	—	—	23.0

[a] For glycerine run 901G conditions of $h_c = 3.16$ mm, $Ca = 2.1$, $Re = 0.66$, $D = 12.7$, and $W = 20.6$. The predicted B for these conditions was 5.7 for all the M and T_0 in Table 1.
[b] Minimum R for this grid occurs at about $T_0 = 0.70 \pm 0.03$ and $M_2 = 1.9 \pm 0.2$.
[c] Fluid properties for glycerine (Lee and Tallmadge, 1972a) were a viscosity of 0.86 N-s/m² (8.6 poise), surface tension of 61.6 N/mm (61.6 dynes/cm), density of 1260 kg/m³, and capillary length of 3.13 mm.

Table 2. Fine Grid Values of R for Glycerine Run 901G Conditions

Parameters			
Slope (M):	1.76	1.85[a]	1.92
Thickness T_0		Values of error integral, $R \times 100$	
0.665	8.0	7.6	9.9
0.681[a]	8.5	7.1[a]	7.6
0.697	10.8	9.6	7.5

[a] Minimum R for this grid occurs at about $T_0 = 0.68 \pm 0.016$ and $M = 1.85 \pm 0.08$.

The pressure profiles for the minimum R conditions for run 901G, shown in Table 2, are those shown in Figure 3. Figure 3c shows how the error function E appeared at the point where iteration was stopped. Thus Figure 3c shows that the normal stress boundary condition was not satisfied exactly for all interfacial positions. However, it is believed that further reductions of the error integral could be made, if desired, by using a more general profile than that of Equation (1). Although a study of the fit of four-parameter and five-parameter equations to data profiles is available (Lee and Tallmadge, 1973a), the increase in computational time and complexity needed for a more general profile would be large and might not improve the accuracy of the predicted profile very much.

COMPARISON OF PREDICTED PROFILES WITH DATA

Comparison of the predicted profile of Equation (9) with experimental data for glycerine run 901G, as shown in Figure 2c, indicates that the numerical prediction is quite close to the data except at the lowest point near the liquid bath level where B is only approximate. Noting that the technique predicts the slope and thickness within 10% and the B intercept within 15%, we conclude that the predicted profile agrees with the data within experimental error. Figure 2c also shows that the two-dimensional flow prediction of this paper is superior to the one-dimensional flow model.

The influence of coating speed on profiles was also studied. To compare with data, the independent conditions were selected as those described by Lee and Tallmadge

TABLE 3. COMPARISON OF PREDICTED PROFILE PARAMETERS WITH DATA FOR OILS

Column	(1) Small *Ca*	(2) Small *Ca*	(3) Larger	(4) Larger	(5) Larger	(6) Smaller	(7) Larger
Name of run	Fluid M	Fluid B	*Ca*	*Ca*	*Ca*	Depth	*Re*
Expt. Cond. (Non Dim).							
Ca no.	0.085	0.48	2.61	5.74	23.9	22.2	3.81
Depth D	17.9	15.1	14.6	15.0	14.7	3.8	5.9
Width W	312	132	56	38	18	19	47
Re no.	0.044	0.016	0.18	0.56	4.84	4.97	12.7
Expt. Cond. (Dim).							
Viscosity, N-s/m^2	0.173	1.05	1.14	1.17	1.17	1.09	0.176
Coating speed, mm/s	15.5	14.6	75	160	671	668	683
Thickness, h_c, mm	0.560	1.33	3.14	4.65	9.52	9.16	3.75
Bath depth, d, mm	10	20	46	70	140	35	22
Bath width, w, mm	175	175	175	175	175	175	175
Run number	224M	318B	311B	308B	303B	313B	216M
Width for Calc, W	36	22	19	38	18	7	13
Profile Intercept, B							
Predicted (one dim)	19	7.5	3.6	2.8	2.6	—	—
Predicted (two dim)	8	6.7	6.5	6.5	6.2	2.4	3.3
Expt. data	13	9.6	6.4	5.2	6.2	2.0	3.2
Profile slope, M							
Predicted (one dim)	2.9	1.78	1.48	1.45	1.40	1.40	1.47
Predicted (two dim)	2.9	2.0	1.8	1.8	2.6	2.5	4.0
Expt. data	4.4	3.2	1.9	1.9	2.4	2.7	4.0
Film Thickness T_0							
Predicted (two dim)	0.61	0.66	0.68	0.69	0.70	0.70	0.68
Expt. data (mass flow)	0.56	0.69	0.71	0.78	0.70	0.67	0.60
Expt. data (micrometer)	0.56	0.67	0.78	0.79	0.77	0.83	0.65

Note A. *Ca* and h_c were calculated using the fluid properties of surface tension and density which are given below as notes C and D.
Note B. The B intercept data for the runs in columns 3 to 5 were reported earlier by Lee and Tallmadge (1973c) for the depth $D = 15$; the column 6 run was reported at depth $D = 4$.
Note C. Fluid properties for fluid B (Lee and Tallmadge, 1972b) were a surface tension of 32.7 N/mm (32.7 dyne/cm), density of 885 kg/m^3, and a capillary length of 2.75 mm.
Note D. Fluid properties for fluid M (Lee, 1974) were a surface tension of 31.5 N/mm (31.5 dyne/cm), density of 874 kg/m^3, and a capillary length of 2.72 mm.

(1972b) for a viscous lubricating oil, called fluid B. At 26.7°C fluid B had a viscosity of 1.31 N-s/m^2 (13.1 poise) and other fluid properties as shown in footnote C of Table 3. Predicted profiles are compared with data in Figures 4a and 4b.

Rectangular plots of these three profiles (Figure 4b) show good agreement with data over the complete profiles. These plots also show that the thick film expression, given by Equation (1), does an excellent job of describing the magnitude of the complete profile so that the thick film parameters are very satisfactory for fitting the thick, thin, and constant regions of the profile. By comparison, the thin film parameters (given as M_1, B_1, and T_0 in Lee and Tallmadge, 1973a) are generally unsatisfactory because of large deviations in the thick, lower region. It was for this reason that the expression based on the thick film was chosen for testing the numerical method of this paper.

Coating speed results for fluid B are shown in columns 3, 4, and 5 in Table 3. For these runs, Table 3 shows good agreement between the two-dimensional predictions of this paper and the data parameters M, B, and T_0. As shown in Table 3, the bath widths used for calculations purposes were generally smaller than the experimental widths in order to reduce computer time; this was done because exploratory tests of the theory at various bath widths indicated little influence on the profiles as long as bath width was larger than bath depth.

The influence of bath depth on intercept B (in other words, profile size) is shown by comparing the shallow bath run (column 6 of Table 3) with the deep bath run (column 5). This comparison shows that the method of this work accurately describes the experimentally observed influence of bath depth on profile size. The data also suggest that varying bath depth does not influence the slope or thickness very much; the two-dimensional predictions for these two runs agree with this observation.

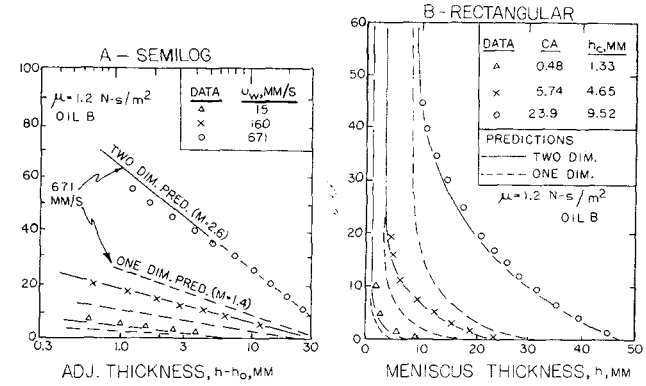

Fig. 4. Comparison of predicted profiles with oil data: (solid lines—two-dimensional model) (dashed lines—one-dimensional model) (data—*B* fluid runs 303*B*, 308*B*, 318*B*)

The influence of a larger Reynolds number is shown in column 7 of Table 3. This run was taken with a less viscous oil, called fluid M, in order to obtain a *Re* larger than the $Re = 5$ of columns 5 and 6. The viscosity of fluid M at 26.7°C was 0.194 N-s/m^2 (1.94 poise) and other fluid properties as shown in footnote D of Table 3. Comparison of intercept and slope in column 7 indicates good agreement of predicted values with data at *Re* of 13.

The only condition for which data-model agreement is not currently satisfactory is for capillary numbers below one. As shown in the column 1 and 2 runs, data-model

differences of about 50% were noted in slopes and intercepts. It is not known whether these differences are due a limitation of the numerical method or not, but it is believed that part of the difference at low Ca is from a larger experimental uncertainty (specifically in determining the position of liquid level) and part is from less accurate numerical results (specifically for the smaller h_0 thicknesses which occur at low Ca). Because mesh size was a fraction of h_0, low Ca runs usually required longer computer time and were stopped with somewhat less accuracy. Nevertheless, the method of this paper does properly predict the functional form of the Ca effect, at Ca below one, namely that both intercept and slope increase when Ca decreases.

Comparison of this work with the unpublished one-dimensional flow model of Lee et al. (1972) for deep baths, as shown in Table 3, indicates that the method of this work predicts an improved profile, especially in terms of the intercept B (in other words, the size of the meniscus). However, the M slopes of Table 3 suggest that the one-dimensional flow model deserves further attention at Ca below one.

RANGE OF THE MODEL

The numerical technique has been tested using profiles and coating thickness for the range of conditions shown in Table 3. The conditions include a six-fold range in viscosity (about 0.2 to 1.2 N-s/m^2) and speeds such that Ca varied from about 10^{-1} to 10^{+1} and Re from about 10^{-2} to 10^{+1}. As shown in Table 3, coating thickness T_0 was quite constant near 0.6 to 0.8 and was closely predicted by the method so that film thickness was not considered to be a sensitive test for this region. Instead, profile parameters B and M were chosen as sensitive tests of the model.

Bath size varied from depths of 10 to 140 mm at a constant width of 175 mm, except for a 65 mm width used in the glycerine run. Thus the nondimensional D was 4 or 15 in the runs. In this range of depth, no effect of the width was found for W of 20 to 300. Depth was therefore considered the primary parameter to describe the effect of bath size.

Based on slope and intercept, Table 3 indicates that the technique developed here is most reliable at Ca above one. The specific range studied was Ca of 1 to 24 and Re of 0.04 to 13. Higher Ca and Re may be feasible up to some limiting value of Re, depending on numerical and hydrodynamic stability.

It is believed that the method would hold at lower Re, provided that Ca were above one. It is also possible that the method could be extended to Ca below one by improving numerical precision, decreasing mesh size, or changing the difference equation techniques. However, a study of such an extension will probably await a need to do so.

DISCUSSION AND SUMMARY

The method of this paper worked well for low Reynolds numbers, but the numerical method became increasingly unstable as the Reynolds number was increased, as expected (Thom and Apelt, 1961). Some of this difficulty could be minimized by the use of the proper grid size or the upwind difference method noted in Gosman et al. (1969).

The evaluation of the flow term in Equation (5) was done numerically as follows:

$$\left(\frac{\partial U_s}{\partial S}\right)_n \simeq \frac{\Delta U_s}{\Delta S} \qquad (10)$$

Because the partial derivative is taken at constant n, the delta terms in Equation (10) were evaluated, as required, along the constant n lines in a n-s mapping plane, that is, along the interface.

Confirmation of the predictive approach by experimental data suggests that the theory can be used to study the effect of feed location, wire withdrawal, and other parameters. The approach also has potential use in other geometries having meniscus flow. The results may also provide a basis, when used with stability analysis, for predicting the onset of some types of film nonuniformities.

In summary, the flow field and meniscus profile have been predicted simultaneously for the first time. The vortex cell and two stagnation points were also observed. The predicted profiles were confirmed by data within experimental error. The method in its current form is recommended for use with free coating at Ca above 1 and Re up to 13 or somewhat higher.

ACKNOWLEDGMENT

This work was sponsored in part by the Eastman Kodak Company. The line diagrams were prepared by William Wasylenko.

NOTATION

b = width of belt, mm
B = meniscus intercept, Equation (1)
c, C = curvature of surface, mm^{-1} and nondimensional
Ca = capillary number, $Ca = \mu u_w/\sigma$
d, D = bath depth, mm, and nondimensional, d/h_c
E = pressure error function, Equation (7)
g = acceleration of gravity, mm/s^2
h = meniscus thickness at any point, mm
h_c = characteristic thickness, $(\mu u_w/\rho g)^{1/2}$, mm
h_0 = coating thickness, constant thickness region, mm
h_v, H_v = distance of vortex cell center from moving wall, mm, and nondimensional, h_v/h_c
L = meniscus thickness, nondimensional, h/h_0
M = meniscus slope, Equation (1)
n = direction normal to the interface
p, P = pressure, N/mm^2, and nondimensional, $(p\ h_c/\mu u_w)$
p_G = pressure in the gas phase, N/mm^2
p_L = pressure in the liquid phase, N/mm^2
R = pressure error integral, nondimensional, Equation (8)
Re = Reynolds number, $h_c u_w \rho/\mu$
s, S = distance along the streamline at the interface, mm, and nondimensional, s/h_c
T_0 = film thickness, nondimensional, $h_0\ (\rho g/\mu u_w)^{1/2}$ or h_0/h_c
u_w = coating or belt velocity, mm/s
u_s, U_s = liquid velocity at the interface in the direction of the interface, mm/s and nondimensional, u_s/u_w
w, W = width of bath, mm, and nondimensional, w/h_c
x, X = vertical coordinate, height above the liquid bath level, mm, and nondimensional (x/h_c)
y, Y = horizontal coordinate, distance from the moving surface, mm, and nondimensional (y/h_c)

Greek Letters

Δ_B = pressure profile, nondimensional, Equation (5)
Δ_F = pressure profile, nondimensional, Equation (6)
λ = meniscus height, nondimensional, x/h_0
μ = liquid viscosity, N-s/m^2
ρ = liquid density, kg/m^3
σ = surface tension of the liquid-air interface, N/mm

LITERATURE CITED

Batchelor, G. K., *An Introduction to Fluid Dynamics*, Chap. 3, Cambridge Univ. Press (1967).

Churchill, S. W., and E. A. Hazhun, "Computation of Three Dimensional Viscous Flow Between Converging Traveling

Surfaces," AIChE Meeting, Minneapolis, Minn. (1972).
Duda, J. L., and J. S. Vrentas, "Fluid Mechanics of Laminar Liquid Jets," *Chem. Eng. Sci.*, **22**, 855 (1967).
Gosman, A. D., W. M. Pun, A. K. Runchal, D. B. Spalding, and M. Wolfstein, *Heat and Mass Transfer in Recirculating Flows*, Academic Press, New York (1969).
Groenveld, P., "High Capillary Number Withdrawal from Viscous Newtonian Liquids by Flat Plates," *Chem. Eng. Sci.*, **25**, 33 (1970).
Groenveld, P., and R. A. Van Dortmond, "Shape of the Air Interface During the Formation of Viscous Liquid Films by Withdrawal," *Chem. Eng. Sci.*, **25**, 1571 (1970).
Gutfinger, C., "Films of Non-Newtonian Fluids in Laminar Motion on Vertical Plates," Ph.D. dissertation, Yale Univ., New Haven, Conn. (1964).
Hirt, C. W., "A Lagrangian Method for Calculating the Dynamics of an Incompressible Fluid with Free Surface," *J. Computational Physics*, **5**, 103 (1970).
Landau, L. D., and V. G. Levich, "Dragging of a Liquid by a Moving Plate," *Acta Physicochim. (U.S.S.R.)*, **17**, 42 (1942).
Lee, C. Y., "Meniscus Flow Fields and Profiles in Free Coating," Ph.D. dissertation, Drexel University, Philadelphia, Pa. (1974).
———., J. J. Braccilli, and J. A. Tallmadge, "Viscous Deformation of Meniscus Profiles," paper presented at Interfacial Phenomena Symp., AIChE Mtg., New York (1972).
Lee, C. Y., and J. A. Tallmadge, "Meniscus Vortexing in Free Coating," *AIChE J.*, **18**, 858 (1972a).
———., "Description of Meniscus Profiles in Free Coating," *ibid.*, 1077 (1972b).
———., "Description of Meniscus Profiles in Free Coating II—Analytical Expression," *AIChE J.*, **19**, 403 (1973a).
———., "Dynamic Meniscus Profiles in Free Coating III—Predictions Based on Two-Dimensional Flow Fields," Symp. Interfac. Phenomena, Joint Meeting of Canadian Inst. of Chem. Eng. and A.I.Ch.E., Vancouver (1973b).
Soroka, A. J., "Continuous Withdrawal of Newtonian Liquid Films on Vertical Plates," Ph.D. Dissertation, Drexel University, Philadelphia, Pa. (1969).
Tallmadge, J. A., and A. J. Soroka, "The Additional Parameter in Withdrawal," *Chem. Eng. Sci.*, **24**, 377 (1969).
Thom, A. A., and C. J. Apelt, *Field Computation in Engineering and Physics*, Van Nostrand, London (1961).
Tuntiblarphol, M., "Obstructed Flow of Newtonian Liquids on Flat Plate Withdrawal," M.S. thesis, Drexel University, Philadelphia, Pa. (1970).

APPENDIX—FLOW FIELD FOR A GIVEN PROFILE

The main purpose of this appendix is to state the boundary conditions and other equations not reported previously (Lee and Tallmadge, 1972a) for the prediction of streamlines in free coating, for the case of a given profile. This concerns Part 1 of the numerical method.

The coating process was described by a steady, two-dimensional flow model. The relevant differential equations were those of continuity and motion for a liquid which has constant density and constant viscosity. They were written with the x direction vertically upward and y horizontal, with the origin at the intersection of the coating surface and the liquid bath surface, and were given in terms of the vertical velocity $u(x, y)$ and horizontal component $v(x, y)$ by (Soroka, 1969; Groenveld, 1970):

$$\frac{\partial u}{\partial x} + \frac{\partial v}{\partial y} = 0 \tag{A1}$$

$$\rho\left[u\frac{\partial u}{\partial x} + v\frac{\partial u}{\partial y}\right] = \mu\left[\frac{\partial^2 u}{\partial x^2} + \frac{\partial^2 u}{\partial y^2}\right] - \frac{\partial p}{\partial x} - \rho g \tag{A2}$$

$$\rho\left[u\frac{\partial v}{\partial x} + v\frac{\partial v}{\partial y}\right] = \mu\left[\frac{\partial^2 v}{\partial x^2} + \frac{\partial^2 v}{\partial y^2}\right] - \frac{\partial p}{\partial y} \tag{A3}$$

Eleven boundary conditions or equations of constraint are applicable to these equations. Referring to Figure 1, six of the boundary conditions (BC's) are no slip of u or v at each of three solid boundaries (continuity of velocity)

$$\text{BC 1 \& 2} \quad u = u_w, \quad v = 0 \quad \text{at} \quad y = 0 \tag{A4}$$

$$\text{BC 3 \& 4} \quad u = 0, \quad v = 0 \quad \text{at} \quad y = w \quad \text{for} \quad -d \leq x \leq 0 \tag{A5}$$

$$\text{BC 5 \& 6} \quad u = 0, \quad v = 0 \quad \text{at} \quad x = -d \tag{A6}$$

Two of the boundary conditions are known velocities for the constant thickness region (Landau-Levich, 1942):

$$\text{BC 7} \quad v = 0 \quad \text{at} \quad x \to \infty \tag{A7}$$

$$\text{BC 8} \quad u = u_w + \left[\frac{h_0^2 \rho g}{2\mu}\right]\left[\left(\frac{y}{h_0}\right)^2 - 2\left(\frac{y}{h_0}\right)\right] \quad \text{at} \quad x \to \infty \tag{A8}$$

The corresponding equation to Equation (A8) in Lee and Tallmadge (1972b) is missing a plus sign. Equations (A7) and (A8) were evaluated by noting that h approaches h_0 asymptotically at infinite height x. Physically, h generally approaches h_0 within a few percent at a height of about $10h_0$ or $20h_0$. Therefore, the numerical formulation for $h = h_0$ is $x > \alpha$ where α is a suitably large distance.

The three remaining equations involve the gas-liquid interface $h(x)$. One is the usual free surface condition of negligible tangential stress

$$\text{BC 9} \quad \tau_{ns} = 0 \quad \text{at} \quad y = h \quad \text{for} \quad 0 \leq x \leq \infty \tag{A9}$$

The second free surface equation of constraint (EC) used here is the assumed shape of the meniscus profile

$$\text{EC 10} \quad h = h(x) \quad \text{assumed} \tag{A10}$$

The third is the result of continuity of net vertical flow across any horizontal cross section of the film, for steady state flow (Landau-Levich, 1942):

$$\text{EC 11} \quad Q = u_w h_0 - \frac{\rho g h_0^3}{3\mu}, \quad \text{or}$$

$$Q = \text{constant} = u_w h_0 \left[1 - (T_0^2/3)\right] \tag{A11}$$

For convenience in solution, the stream function and vorticity were introduced in the standard way. The pressure and gravity terms were eliminated by differentiation to obtain one fourth-order, motion equation. Choosing wall speed u_w and thickness h_c as characteristic speed and length, respectively, the differential motion equation was obtained in terms of the nondimensional stream function ψ and nondimensional vorticity ω

$$\left[\frac{\partial \psi}{\partial Y}\frac{\partial \omega}{\partial X} - \frac{\partial \psi}{\partial X}\frac{\partial \omega}{\partial Y}\right] = \frac{1}{Re}\left(\frac{\partial^2 \omega}{\partial Y^2} + \frac{\partial^2 \omega}{\partial X^2}\right) \tag{A12}$$

$$-\omega = \frac{\partial^2 \psi}{\partial Y^2} + \frac{\partial^2 \psi}{\partial X^2} \tag{A13}$$

Equation (A13) is the vorticity equation. The equations of constraint and boundary conditions in ψ, ω form have appeared elsewhere (Lee and Tallmadge, 1972b). These elliptic equations (A12) and (A13) were written in difference equations and then solved for a fixed boundary by an iterative successive substitution technique using central differences in the bulk and special equations at the surfaces (Lee, 1974). The numerical method worked well for the low Reynolds numbers studied here, namely, where $Re < 50$. Other details are given in Lee and Tallmadge (1972b) and Lee (1974).

The pressure profile terms of Equation (6), $\partial P/\partial X$ and $\partial P/\partial Y$, were evaluated using

$$-\frac{\partial P}{\partial X} = \frac{\partial \omega}{\partial Y} + Re\left[\frac{\partial \omega}{\partial Y}\frac{\partial^2 \psi}{\partial X \partial Y} - \frac{\partial \psi}{\partial X}\frac{\partial^2 \psi}{\partial Y^2}\right] + 1 \tag{A14}$$

$$+\frac{\partial P}{\partial Y} = \frac{\partial \omega}{\partial Y} + Re\left[\frac{\partial \psi}{\partial Y}\frac{\partial^2 \psi}{\partial X^2} + \frac{\partial \psi}{\partial X}\frac{\partial^2 \psi}{\partial X \partial Y}\right] \tag{A15}$$

Other details of this solution are given in Lee (1974).

Manuscript received September 4, 1973; revision received May 14 and accepted June 11, 1974.